Available online at www.sciencedirect.com
SCIENCE DIRECT®
Journal of Nuclear Materials 329–333 (2004) 1575–1579
journal of nuclear materials
www.elsevier.com/locate/jnucmat

# Desorption of water from iron oxide by laser irradiation

K. Chiba *, S. Tanaka, T. Yoneoka

*Department of Quantum Engineering and System Science, The University of Tokyo, 7-3-1 Hongo Bunkyo-ku, Hongo, Tokyo 113-8656, Japan*

**Abstract**

Desorption of water adsorbed on iron oxide by laser irradiation was studied by means of a time-of-flight (TOF) technique. Laser wavelength of $\lambda = 355$ and 430 nm were used. The dependence of the velocity distribution of desorbed water on the temperature (246–324 K) of the iron oxide and on the adsorption state of water were investigated. The desorption mechanism of water from the iron oxide which is in the form of OH is not dependent on the temperature (246–324 K) of the iron oxide. The desorption by laser irradiation at $\lambda = 430$ nm from iron oxide on which water is molecularly adsorbed on the surface OH at 229 K is considered to be initiated by the two series of steps: (1) surface OH captures the electron excited in the iron oxide and gains kinetic energy; (2) this energy transfers to the water molecules which are molecularly adsorbed near this OH.


## 1. Introduction

It is well known that tritium is easily adsorbed on the surface of structural materials in the tritium handling system. From the viewpoint of tritium safety in a fusion reactor, an effective method of removing adsorbed tritium is needed and several techniques have been proposed [1–8]. Irradiation by energetic particles (electrons, or ions) or photons of the surface of contaminated materials has been proposed as an effective method to remove tritium and the effect of this method has been investigated [3–8]. However, the fundamental desorption mechanism remains to be elucidated. Much research has been carried out on the desorption mechanisms of species adsorbed on the surface induced by irradiation with energetic particles or photons in various systems [9–15]. However, these experiments were conducted under ideal conditions, such as a highly evacuated surface or a cleaned surface. It is necessary to elucidate the desorption mechanism in actual conditions, such as a surface covered with oxide or organic matter.

In order to determine the desorption mechanism induced by laser irradiation, it is useful to analyze the velocity distribution of the desorbed species and the dependence of desorption behavior on the photon energy [12–15]. This is because the velocity distribution and the dependence of desorption behavior on the photon energy give important information about the desorption mechanism. In our previous study [8], we obtained the velocity distribution of the desorbed species from surface OH by photon irradiation using pulse lasers and a time-of-flight (TOF) technique. Our findings suggested that the main species desorbed by laser irradiation was water and that the desorption of water from the surface of iron oxide was caused not only by a thermal process via the rise of the surface temperature but also by a nonthermal process that followed electron transfer from the iron oxide to the adsorbed hydroxyl. The thermal process following laser irradiation was dominant at $\lambda = 355$ nm. On the other hand, the nonthermal process was dominant at $\lambda = 430$ nm. In order to elucidate the detailed desorption mechanism, investigation of the dependence on the temperature of the surface and the adsorption state of water is important.

* Corresponding author. Tel.: +81-3 5841 6970; fax: +81-3 3818 3455.
*E-mail address:* kunihiko@flanker.q.t.u-tokyo.ac.jp (K. Chiba).

0022-3115/$ - see front matter © 2004 Published by Elsevier B.V.
doi:10.1016/j.jnucmat.2004.04.167

These studies are also important because in actual conditions the temperature of the materials and the adsorption state of tritium is not uniform. In the present study, the dependence of the desorption mechanism on the temperature of the iron oxide and the amount of the adsorbed water was investigated.

## 2. Experimental

Desorption experiments were carried out in a vacuum chamber for TOF analysis. A tunable laser (pulse duration = 4–6 ns) irradiated the sample surface at 45° from the sample normal for desorption. In this study, laser wavelength of $\lambda = 355$ (3.5) and 430 nm (2.9 eV) were used for desorption. The typical laser spot size on the surface was about 0.3 $cm^2$ and the laser power was 2.5 $mJ/cm^2$. The laser shot repetition rate was 10 Hz. The species desorbed by the laser irradiation for desorption was ionized using a fourth harmonic of a Nd:YAG laser (pulse duration = 4–6 ns, 266 nm, 45 mJ/pulse) focused by a quartz lens with a focal length of 300 mm. The distance between the sample and the laser for ionization was 4 mm. These ions were accelerated to the flight tube and then detected by a micro-channel plate (MCP) assembly. The mass of these ions was evaluated from the time required to traverse the distance between the ionization region and the MCP. In this system, $m/e = 17$ is discriminated from $m/e = 18$. The velocity distribution of the desorbed species was obtained by varying the delay time between the laser for desorption and the laser for ionization. Details of the experimental system are reported elsewhere [8].

A plate of pure iron (99.9%, length: 40 mm, width: 10 mm, thickness: 0.5 mm) was used as a specimen in the present study. Electrolytic polishing (phosphoric acid, 10 min) and oxidation of the sample surface (673 K, $O_2$ 20 Pa, for 1 h) were conducted. By this treatment, a thin layer of the iron oxide, mainly $Fe_2O_3$, grew on the surface. The details of the preparation of the sample are reported elsewhere[8]. The sample surface was directly exposed to liquid $H_2O$ in air for 3 h at room temperature. Before the sample was irradiated with the laser for desorption, the chamber was evacuated to about $10^{-4}$ Pa. When the residual gas in the chamber was detected using QMS, the main gas was water vapor.

For temperature dependence experiments, after exposure to $H_2O$ the sample was placed in the vacuum chamber at 296 K, then the sample temperature was controlled at 246 K (called S1 in this paper), 296 K, and 324 K. From UPS analysis, it was found that water was dissociatively adsorbed on the sample surface and hydroxyls were formed at room temperature; after heating to 473 K in vacuum these hydroxyls remained on the surface [5]. Molecularly adsorbed water was not observed on the surface. In the case of S1, water was considered to be adsorbed on the surface as hydroxyls because the sample was cooled after placing the sample in the vacuum chamber.

The sample preparation for experiments on the dependence of the adsorption state of the water was as follows. The sample was cooled to about 267 K (below freezing) in air after $H_2O$ exposure. By this treatment, ice layers were formed on the surface. After that, this sample was placed in the vacuum chamber with the sample temperature kept below 267 K during evacuation. The sample temperature was 246 or 229 K during the irradiation by the laser at $\lambda = 355$ or 430 nm. This sample is designated in this paper as S2. Compared with S1 which was cooled after placing the sample in the vacuum chamber at 296 K, the amount of water adsorbed on the surface of S2 would be large and the molecularly adsorbed water was assumed to exist on the surface.

## 3. Results and discussion

### 3.1. Dependence on the sample temperature

Fig. 1 shows the velocity distributions (Fig. 1(a)) of the water desorbed from the surface OH by the laser irradiation at $\lambda = 355$ nm at 246, 296 and 324 K, and the desorption yield (Fig. 1(b)) as a function of the laser power at 246 and 324 K. $m/e = 18$ signal detected by MCP was bigger than $m/e = 17$. Therefore, the main species desorbed by the laser irradiation were water molecules. The surface OH is considered to combine with nearby OH to form $H_2O$, and this $H_2O$ is desorbed. The dependence of the desorption yield of water by laser irradiation at $\lambda = 355$ nm at 246 and 324 K on the laser power was nearly exponential. These results consistent with that of a sample on which water was adsorbed as surface OH at room temperature [8]. This suggests that the desorption is caused by a thermal process. This is because the desorption yield by the thermal process depends on $\exp(-E/k(T + dT))$, where $E$ is activation energy, $k$ Boltzmann constant, $T$ the sample temperature before laser irradiation and $dT$ the temperature rise following laser irradiation, which is considered to be nearly proportional to the laser power. The velocity distributions of the water desorbed by laser irradiation at $\lambda = 355$ nm were well fit by a Maxwell–Boltzmann distribution ($f(v) = Av^2 \exp(-Bv^2)$), as shown in Fig. 1(a). The dependence on laser power and the analysis of the velocity distribution indicate that in the case of $\lambda = 355$ nm the thermal process via the rise of the surface temperature following the laser irradiation is the dominant process for the desorption of water at 246, 296 and 324 K. As shown in Fig. 1(a), the velocity distribution shifted to higher velocity with increasing sample temperature and the temperatures ($T = m/2kB$) esti-

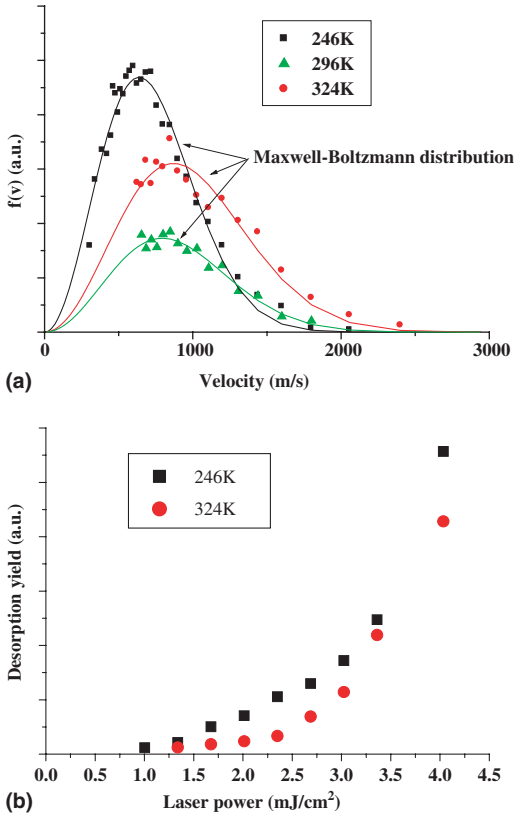


Fig. 1. Temperature dependence of water desorbed by laser irradiation at $\lambda = 355$ nm. (a) The velocity distribution. (b) Desorption yield as a function of laser power.

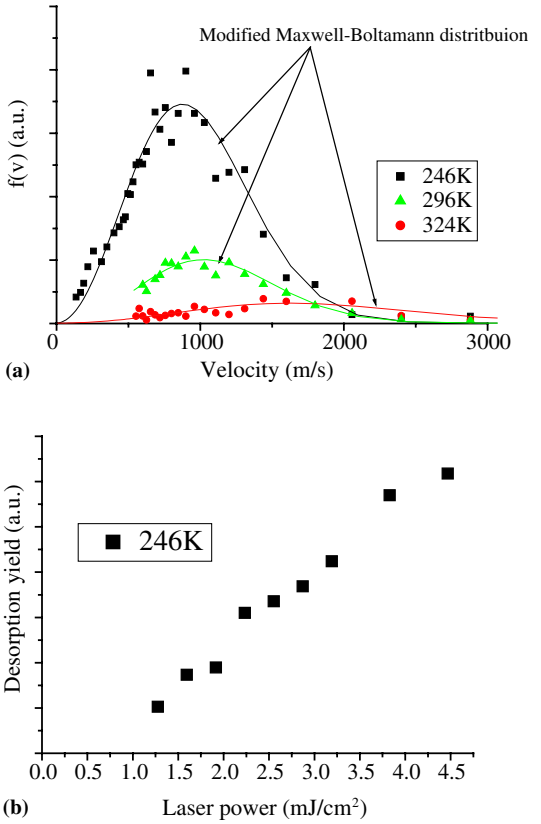


Fig. 2. Temperature dependence of water desorbed by laser irradiation at $\lambda = 430$ nm. (a) The velocity distribution. (b) Desorption yield as a function of laser power at 246 K.

mated from the Maxwell–Boltzmann fitting at 246, 296 and 324 K were 440, 690 and 820 K, respectively. This is because the water desorbed via the thermal process is in equilibrium with the surface and the surface temperature following laser irradiation is considered to be higher than before the laser irradiation.

Fig. 2 shows velocity distributions (Fig. 2(a)) of the water desorbed by laser irradiation at $\lambda = 430$ nm at 246, 296 and 324 K from the surface on which water is adsorbed as surface OH, and the desorption yield (Fig. 2(b)) as a function of the laser power at 246 K. The desorption yield by laser irradiation at $\lambda = 430$ nm at 246 K is nearly proportional to the laser power. This result was consistent with that of the sample on which water was adsorbed as surface OH at room temperature [8]. The velocity distributions of the desorbed water were well fit by a modified Maxwell–Boltzmann distribution ($f(v) = Av^2 \exp(-B(v - v_0)^2)$) [11,16]. This functional form was used for representing the velocity distribution of the particles desorbed from the surface after obtaining kinetic energy via the nonthermal process [11–15]. In the case of $\lambda = 430$ nm the nonthermal process appears to be the dominant process for desorption at 246, 296 and 324 K. This is because the desorption is mainly caused by a single photon process and not by the thermal process. This nonthermal process at 296 K is initiated by electronic excitation from the valence band to the conduction band in the iron oxide under laser irradiation as reported elsewhere [8]. The excited electron in the iron oxide is captured by the surface OH from the iron oxide and negative ionic state is generated on the surface. This formation of the ionic state promotes the nonthermal desorption. The detailed desorption mechanism was discussed in our previous studies [5,8]. The desorption of water via this mechanism is also considered to occur at 246 and 324 K. This is because water is adsorbed on the surface as OH at these temperatures as well as at 296 K. As shown in Fig. 2(a), the velocity distribution shifted to higher velocity with increasing sample temperature. The velocity of the water desorbed via the nonthermal process appears to depend on the surface temperature and is higher with increasing surface temperature. Compared with the velocity distributions at $\lambda = 355$ nm, the velocity distributions at $\lambda = 430$ nm were shifted to higher velocity at each

temperature. This is because the water desorbed via the nonthermal process gains kinetic energy by electron transfer from the iron oxide to the OH and this water is considered to have higher energy than the water desorbed via the thermal process.

### 3.2. Dependence on the adsorption state of water on the surface

The velocity distributions of the water desorbed by laser irradiation at $\lambda = 355$ nm from S1 and S2 are shown in Fig. 3(a). The amount of water desorbed from S2 was larger than that from S1, while the peak position of the velocity distribution of S2 was similar to that of S1. These velocity distributions were well fit by a Maxwell–Boltzmann distribution and the dependence of the desorption yield from S1 and S2 on the laser power was nearly exponential (Fig. 3(b)). From these results, it appears that in the case of $\lambda = 355$ nm the desorption mechanism of the water from S1 and S2 is mainly thermal process, which is independent of the adsorption state of water; i.e., surface OH or molecularly adsorbed water. Since the photon energy of a laser with $\lambda = 355$ nm cannot directly excite an electron of the adsorbed water [8], the thermal process is considered to be caused by the rise of the surface temperature following laser irradiation. The photon penetration depth is on the order of $10^{-8}$ to $10^{-7}$ m [10], and the rise of the surface temperature is considered to occur within this depth. Since the layer of the water adsorbed on the sample surface under these experimental conditions is considered to be much thinner than the penetration depth, the amount of adsorbed water does not affect the temperature rise following laser irradiation. Therefore, the peak position in the velocity distribution of S1 is similar to that of S2, because the temperature of S2 following laser irradiation is nearly equivalent to that of S1.

The velocity distributions of the water desorbed by laser irradiation at $\lambda = 430$ nm from S1 and S2 are shown in Fig. 4(a). The amount of water desorbed from S2 was larger than that from S1, and the shape of the velocity distribution of S1 was different from that of S2. As shown in Fig. 4(b), the desorption yield of S2 was not linearly dependent on the laser power and increased

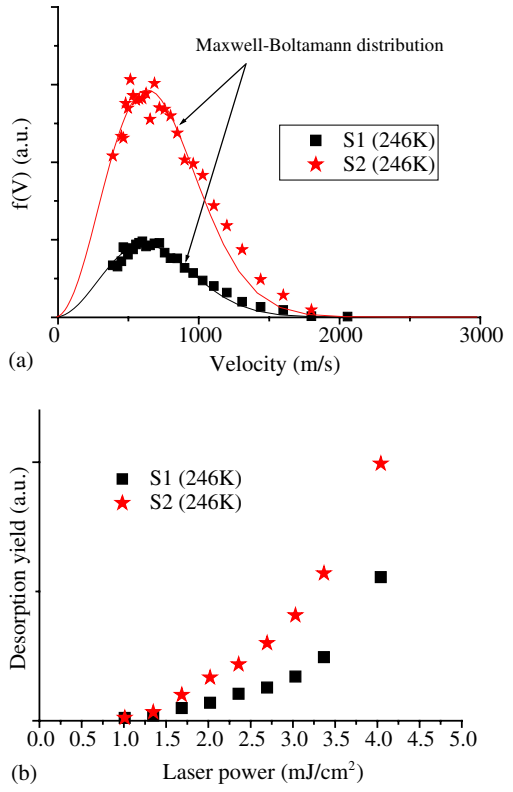


Fig. 3. Dependence of water desorbed by laser irradiation at $\lambda = 355$ nm on the adsorption state of water. (a) The velocity distribution. (b) Desorption yield as a function of laser power. About S1 and S2, see the text.

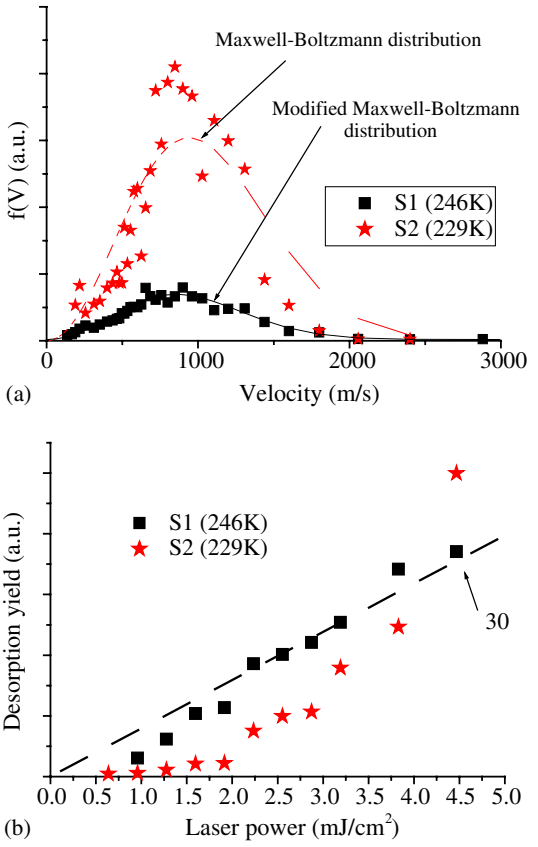


Fig. 4. Dependence of water desorbed by laser irradiation at $\lambda = 430$ nm on the adsorption state of water. (a) The velocity distribution. (b) Desorption yield as a function of laser power. About S1 and S2, see the text.

rapidly at larger laser powers. On the other hand, the desorption yield of S1 was linearly dependent. These results imply that the desorption mechanism from S2 is different from the nonthermal process of S1. A fit of the S2 velocity distribution to the Maxwell–Boltzmann distribution was attempted, but the fitting result was not consistent with the experimental results as shown in Fig. 4(a). This implies that the desorption mechanism of water from S2 is not a thermal process and the desorbed water is not in equilibrium with the surface. Wolf [12] reported that water adsorbed on Pd(1 1 1) below one layer was desorbed via a photochemical process such as electron transfer by laser irradiation, and multilayers of adsorbed water prevented the desorption of water from the first layer. If water is molecularly adsorbed on the surface OH by hydrogen bonding, the energy which the surface OH gained through electron capture from the iron oxide could be transferred to the nearby water. The water molecules which gain energy from the OH are considered to be easily desorbed, because the binding energy of this water is small compared with that of the adsorbed OH. Therefore the amount of the water desorbed from S2 is larger than that from S1. The water desorbed via such a mechanism is not in equilibrium with the surface. This is because the desorption of water occurs before these water molecules thermally equilibrate with the surrounding adsorbed water. As a result, the velocity distribution of water desorbed from S2 did not exhibit Maxwell–Boltzmann distribution.

## 4. Conclusions

The dependence of the velocity distribution on temperature (246–324 K) of the iron oxide and the adsorption state of water suggest the following mechanisms for desorption of water by laser irradiation at $\lambda = 355$ and 430 nm:

(1) The desorption mechanism of the water from the iron oxide on which water is adsorbed as surface OH is not dependence on the temperature (246–324 K) of the iron oxide. A thermal process is dominant for $\lambda = 355$ nm, and a nonthermal process is dominant for $\lambda = 430$ nm. The velocity distribution shifts to higher velocity with increasing sample temperature at $\lambda = 355$ and 430 nm.

(2) The desorption of water by laser irradiation at $\lambda = 355$ nm from the iron oxide which is molecularly adsorbed by hydrogen bonding with surface OH at 246 K is mainly caused by the thermal process. The peak position of velocity distribution of the water desorbed via the thermal process is independent of the adsorption state.

(3) The desorption of water which is molecularly adsorbed by hydrogen bonding with surface OH at 229 K by laser irradiation at $\lambda = 430$ nm from the iron oxide is initiated by the two series of steps: (1) surface OH captures the electron excited in the iron oxide and gains kinetic energy; (2) this energy is transferred to the water molecules which are adsorbed molecularly nearby. These water molecules are desorbed before they thermally equilibrate with the surrounding water.

## References

[1] N. Masaki, T. Hirabayashi, M. Saeki, Fus. Technol. 15 (1989) 1337.
[2] J.P. Krasznai, R. Mowat, Fus. Technol. 28 (1995) 1336.
[3] Y. Oya, T. Tadokoro, W. Shu, T. Hayashi, S. O'hira, M. Nishi, J. Nucl. Sci. Technol. 38 (2001) 967.
[4] K. Chiba, T. Yoneoka, S. Tanaka, Fus. Technol. 39 (2001) 1038.
[5] K. Chiba, R. Sato, T. Yoneoka, S. Tanaka, Fus. Sci. Technol. 41 (2002) 386.
[6] K. Chiba, R. Sato, T. Yoneoka, S. Tanaka, Fus. Eng. Des. 61&62 (2002) 775.
[7] K. Chiba, R. Ohmori, T. Yoneoka, S. Tanaka, Phys. Scr. T 103 (2003) 125.
[8] K. Chiba, S. Tanaka, T. Yoneoka, J. Nucl. Mater., to be published.
[9] T.J. Chuang, Surf. Sci. Rep. 3 (1983) 1.
[10] X.-L. Zhou, X.-Y. Zhu, J.M. White, Surf. Sci. Rep. 13 (1991) 73.
[11] F.M. Zimmermann, W. Ho, Surf. Sci. Rep. 22 (1995) 127.
[12] M. Wolf, S. Nettesheim, J.M. White, E. Hasselbrink, G. Ertl, J. Chem. Phys. 94 (1991) 4609.
[13] X.-Y. Zhu, J.M. White, M. Wolf, E. Hasselbrink, G. Ertl, J. Phys. Chem. 95 (1991) 8393.
[14] K. Fukutani, A. Peremans, K. Mase, Y. Murata, Surf. Sci. 283 (1993) 158.
[15] K. Fukutani, Y. Murata, R. Schwarzwald, T.J. Chung, Surf. Sci. 311 (1994) 247.
[16] F. Budde, T. Gritsch, A. Modl, T.J. Chuang, G. Ertl, Surf. Sci. 178 (1986) 798.